

Natural history of severe decompression sickness after rapid ascent from air saturation in a porcine model

DAVID M. DROMSKY,¹ CHARLES B. TONER,¹ SHALINI SURVANSI,¹ ANDREAS FAHLMAN,² ERICH PARKER,¹ AND PAUL WEATHERSBY¹

¹Naval Medical Research Center, Bethesda, Maryland 20889-5607; and ²Department of Biology, Carleton University, Ottawa, Ontario, Canada K1S 5B6

Received 6 December 1999; accepted in final form 1 March 2000

Dromsky, David M., Charles B. Toner, Shalini Survanshi, Andreas Fahlman, Erich Parker, and Paul Weathersby. Natural history of severe decompression sickness after rapid ascent from air saturation in a porcine model. *J Appl Physiol* 89: 791–798, 2000.—We developed a swine model to describe the untreated natural history of severe decompression sickness (DCS) after direct ascent from saturation conditions. In a recompression chamber, neutered male Yorkshire swine were pressurized to a predetermined depth from 50–150 feet of seawater [fsw; 2.52–5.55 atmospheres absolute (ATA)]. After 22 h, they returned to the surface (1 ATA) at 30 fsw/min (0.91 ATA/min) without decompression stops and were observed. Depth was the primary predictor of DCS incidence ($R = 0.52$, $P < 0.0001$) and death ($R = 0.54$, $P < 0.0001$). Severe DCS, defined as neurological or cardiopulmonary impairment, occurred in 78 of 128 animals, and 42 of 51 animals with cardiopulmonary DCS died within 1 h after surfacing. Within 24 h, 29 of 30 survivors with neurological DCS completely resolved their deficits without intervention. Pretrial Monte Carlo analysis decreased subject requirement without sacrificing power. This model provides a useful platform for investigating the pathophysiology of severe DCS and testing therapeutic interventions. The results raise important questions about present models of human responses to similar decompressive insults.

saturation; diving; swine; dose response

WHEN AN AIR-BREATHING ORGANISM is exposed to depth, the elevated ambient pressure dissolves inert respiratory gases, chiefly nitrogen, into the organism's tissues. Under pressure, this uptake continues until equilibrium occurs, at which point the organism is said to be saturated. After hyperbaric exposures, divers return to normal pressure in carefully calculated increments. This process, called decompression, allows gradual, safe elimination of inert gases from the tissues. When decompression happens too quickly, the liberated gas forms bubbles that can block blood vessels and damage tissue, producing the medical condition called decompression sickness (DCS). After saturation, the tissues contain the maximum nitrogen load possible for a

given depth, so decompression from saturation exposures is a lengthy, intensive process.

However, plausible situations may require humans to conduct a direct ascent from saturation conditions. The US Navy almost never experiences accidents that leave their submarines disabled, but when they do, such accidents pose a difficult rescue problem. Submarines are maintained at normal atmospheric pressure, but over time the pressure within a disabled submarine is expected to rise because of a variety of factors. While awaiting rescue, the sailors' tissues will most likely become saturated with nitrogen from breathing air at the elevated pressure. Rescue efforts may not allow a proper, controlled decompression, and ready access to a recompression chamber cannot be guaranteed. DCS sustained in this situation could potentially cause severe long-term morbidity and mortality. This operational possibility was the impetus for conducting this trial.

Predicting the exact DCS incidence and severity after such ascents is difficult. Extant human dive trial data on direct ascent from saturation conditions are relatively sparse and, for ethical reasons, do not approach the severe profiles possible in such rescue situations (2, 10, 11, 29). Previous experience has suggested that direct ascent to the surface from saturation depths deeper than 30 feet of seawater (fsw) may result in morbidity levels that would make human experimental exposures impossible. USN 93, a probabilistic computer model calibrated with a database of 3,322 dives, projects a very gradual rise in DCS incidence after direct ascent from saturation, moving from 25 to 75% incidence over a saturation depth range of 40–120 fsw [2.21–4.64 atmospheres absolute (ATA)] (26). The model's calibration data set includes ~600 saturation dives but none followed by direct ascent exceed 30 fsw (1.91 ATA). Thus, for deeper exposures, the model is extrapolating outside its calibration data set, so those predictions may be suspect.

We designed this experiment to describe the manifestations of severe DCS after direct ascent from saturation conditions in a large-animal model and to define

Address for reprint requests and other correspondence: D. M. Dromsky, Code 031, Naval Medical Research Center, 8901 Wisconsin Ave., Bethesda, MD 20889-5607 (E-mail: dromskyd@nmriponmri.nmrc.navy.mil).

The costs of publication of this article were defrayed in part by the payment of page charges. The article must therefore be hereby marked "advertisement" in accordance with 18 U.S.C. Section 1734 solely to indicate this fact.

a high-incidence point for future therapeutic intervention trials. Initially a search for the 75% incidence point with use of 40 animals, the study broadened into observation of a full dose-response curve including 128 animals. The decompression was sufficiently short that nitrogen washout could hardly begin before observation at the surface. The results bear on preparations for emergency situations that may expose humans to similar stress.

MATERIALS AND METHODS

All procedures were conducted in accordance with National Research Council guidelines on laboratory animal use (20). Before the study, the Institutional Animal Care and Use Committee reviewed and approved all aspects of the protocol. The institutional animal care facility is fully certified by the American Association for Accreditation of Laboratory Animal Care.

Animals. Neutered male Yorkshire swine littermates from a closed breeding colony [$n = 128$; 20.0 ± 1.71 (SD), range 17.1–24.8 kg body wt] were examined by a veterinarian on receipt, fitted with an adjustable chest harness, and housed in individual runs where water was freely available. Their daily feedings consisted of 2% by body weight laboratory animal feed (Harlan Teklad, Madison, WI). Animals remained in the care facility for ≥ 72 h to adjust to their new surroundings before experiments.

Pre-dive preparation. Animals were brought to the laboratory in plastic transport kennels ($22 \times 32 \times 22$ in., Vari-Kennel, R. C. Steele, Brockport, NY), placed in a Panepinto sling (Charles River, Wilmington, MA), and anesthetized by intramuscular injection of 20 mg/kg ketamine and 1 mg/kg xylazine. By use of sterile technique, 10 cm of a customized Micro-Renathane catheter (model RPC-040, Braintree Scientific, Braintree, MA) were inserted into an ear vein and lightly tied in place to provide ready peripheral venous access. After the incision was closed, the catheter was connected to an injection port. Animals then received 500 mg of chloramphenicol to reduce infection risk and 1 ml of heparinized saline (2 U/ml) to maintain catheter patency overnight. The catheter was sutured to the ear and taped down with waterproof surgical tape. After complete recovery, animals were returned to the care facility.

Procedure. On the morning after catheterization, animals were brought to the laboratory and placed in a Panepinto sling, where they received another 1 ml of heparinized saline (2 U/ml). They were then weighed and put in a modified transport kennel that allowed direct visualization of the animal throughout the dive.

Animal pairs were placed in a computer-controlled hyperbaric chamber (5.6-m³ internal volume, WSF Industries, Buffalo, NY) and compressed to a preselected depth with air. Compression progressed in phases, beginning with 5 fsw/min to a depth of 33 fsw (2 ATA). If the animal showed no distress or other evidence of middle ear barotrauma, we increased descent rate to 10 fsw/min down to 99 fsw (4 ATA). If the animal again tolerated the descent well, we increased descent to 20 fsw/min down to the final depth. Animal comfort was the limiting factor in all descent rates. Temperature was maintained between 26.7 and 29.4°C, humidity between 50 and 75%, and CO₂ concentration below 0.3%. The animals were constantly monitored via closed-circuit television cameras through observation ports. After 22 h, the animals were returned to the surface (1 ATA) at a nominal rate of 30 fsw/min with no decompression stops. In practice, that rate

was closely followed until a depth of ~ 15 fsw (1.45 ATA). Because of piping restrictions, the remainder of the decompression required 60–70 s.

On reaching the surface (1 ATA), the animals were fitted with individual monitors that measured heart rate and Hb saturation (VetOx 4404, Heska, Ft. Collins, CO) and then transferred to individual $36 \times 23 \times 22$ -in. clear Plexiglas observation pens. Onset of severe DCS (neurological or cardiopulmonary dysfunction) was recorded to the nearest minute. Disease and symptom onset times were referenced to the time animals reached the surface. Neurological DCS was defined as motor weakness (diminished limb strength, repeated motor incoordination, or inability to stand after being righted by the investigator), paralysis (complete limb dysfunction, areflexia, or hypotonia), or cranial nerve dysfunction. Cardiopulmonary DCS was defined as a visually observed respiratory rate >90 breaths/min combined with respiratory distress, as evidenced by open-mouth, labored breathing, central cyanosis, inversion of the normal inspiratory-to-expiratory ratio, and production of frothy white sputum. All animals with signs of severe DCS were removed to a Panepinto sling and given 2.5 mg of diazepam iv as necessary to alleviate their distress. Skin DCS and behavioral features (e.g., limb lifting) indicative of milder DCS were noted but not classified as positive cases for this study. After the 1-h observation period the animals were weighed. Close observation continued until 4 h after they reached the surface, at which time they were returned to the care facility. Animals were examined again 24 h later, anesthetized with an intravenous injection of 20 mg/kg ketamine and 1 mg/kg xylazine, and then euthanized by cardioplegia with a bolus intravenous injection of 40 ml of 4 M potassium chloride solution.

All animals that developed severe DCS or expired from their disease were immediately sent for necropsy. The viscera were removed, and the heart was examined for patent foramen ovale. The heart, lungs, brain, and spinal cord were removed and examined grossly. Tissues were preserved in Formalin. Representative sections of cervical, thoracic, lumbar, and sacral spinal cord, brain stem, cerebellum, cerebrum, and lung were embedded in paraffin. Sections were cut at 6 μ m, stained with hematoxylin and eosin, and examined under light microscopy by a veterinary pathologist.

Analysis. Data were analyzed by logistic regression with maximum-likelihood parameter estimation in the manner described by Hosmer and Lemeshow (17). Significance of specific independent variables was determined using the likelihood ratio test. Resultant dose-response curves were plotted using the logistic regression equation incorporating all significant independent variables

$$\log[P/(1 - P)] = \beta_0 + \beta_1 * \text{var}_1 + \dots + \beta_n * \text{var}_n$$

where β_0 is intercept and β_n is the parameter associated with the respective variable.

RESULTS

Initially 40 animals were used according to the decision rules outlined in the trial design (see APPENDIX), and a dose-response curve was plotted (Fig. 1). This preliminary modeling effort predicted the 75% incidence near 110 fsw (4.33 ATA). We subjected 36 additional animals to dives at that depth to define it for use in future intervention studies. The resulting incidence at 110 fsw (4.33 ATA) was 68% (95% confidence interval = 52–81), which is very close to the preliminary prediction. We subjected 24 animals to dives at shall-

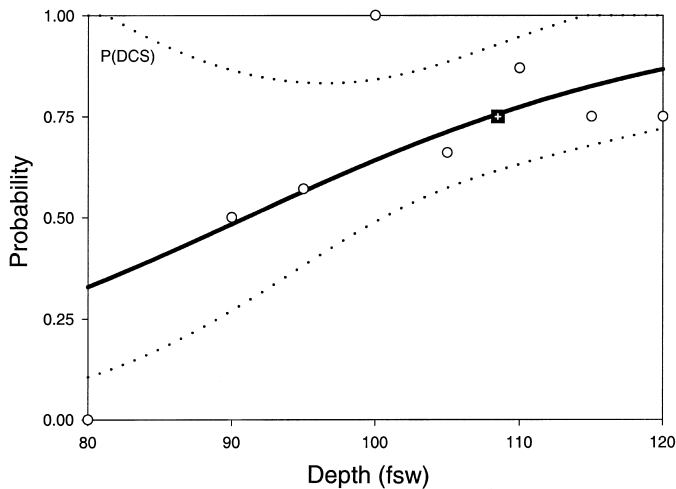


Fig. 1. Dose-response curve after initial cohort. The logistic regression plot of decompression sickness (DCS) incidence is based on the outcomes of 40 subjects with 95% model confidence limits. \circ , Observed incidence at each depth; cross enclosed in square, the predicted 75% incidence point. $\beta_0 = -5.89$, $\beta_1 = 0.0647$. fsw, Feet of seawater.

lower depths in support of ongoing interspecies scaling efforts. Finally, 28 animals were used to define the highest-incidence regions. Figure 2 shows the final dose-response curves for severe DCS and death as derived by logistic regression with model 95% confidence limits.

Table 1 lists the mean times to diagnosis of DCS and death. Overall, 81 of 128 animals developed severe DCS [18.1 ± 13.0 (SD) min], and 43 of 128 died from their disease (26.1 ± 12.0 min). Onset of severe DCS and death varied widely. Some animals with DCS manifested signs very quickly, whereas other animals on the same dive showed no evidence of DCS. Figure 3 relates the percentage of surviving animals as a function of time to different depth profiles. Note that as depth increases, disease latency and overall survival decrease.

Outcome was analyzed by logistic regression with maximum-likelihood parameter estimation. Independent variables included animal age, pre-dive weight, dive depth, and weight loss during the dive. Table 2 contains parameters and their respective measures of significance for a regression of all independent variables. Likelihood ratio testing identified increasing depth as the only significant determinant of DCS incidence ($\beta = 0.083$, $P < 0.0001$). Significant factors in predicting death incidence included depth ($\beta = 0.088$, $P < 0.0001$) and pre-dive weight ($\beta = 0.305$, $P = 0.0361$).

Neurological DCS. The neurological DCS encountered in this model usually appeared <1 h after the animals surfaced and developed rapidly over the course of a few minutes. It manifested as progressive weakness of one or more limbs, most commonly hind-limb dysfunction or frank paralysis. A greater proportion of isolated central nervous system (CNS) DCS occurred on profiles below the 50% incidence depth of 102 fsw (4.09 ATA) ($\chi^2 = 9.24$, $P = 0.0024$). More CNS cases presented beyond that point but often in combi-

nation with cardiopulmonary DCS that was sometimes so fulminant that the animal succumbed before objective evidence of a localized CNS event could be confirmed. Most animals with evidence of neurological DCS began to show recovery within the 4-h observation period, and all but one animal that survived decompression were deficit free and normal to examination at the 24-h observation. Interestingly, the only case that did not resolve by 24 h was also the only one that presented >1 h after reaching the surface.

Cardiopulmonary DCS. Cardiopulmonary DCS was commonly observed in these dive profiles, occurring in 53 of 81 cases. As noted above, most of the cases occurred at or beyond 100 fsw (4.03 ATA). Cases presented as progressive tachypnea and tachycardia with Hb saturation $<80\%$, despite respiratory rates $>300\%$ of baseline and heart rates $\sim 200\%$ of baseline, and were often accompanied by production of frothy white sputum and open-mouth, labored respiration. Ten an-

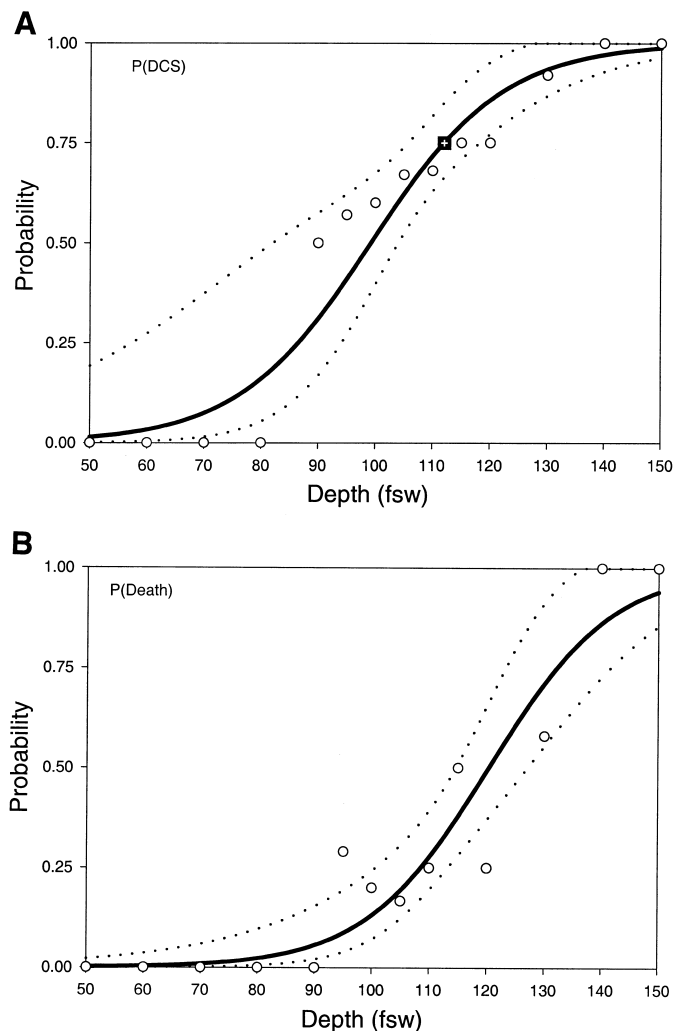


Fig. 2. Final dose-response curves. The logistic regression plot of severe DCS and death incidence is based on the outcomes of 128 subjects with 95% model confidence limits with use of all significant variables from Table 2. \circ , Observed incidence at each depth; cross enclosed in square, the predicted 75% incidence point. The curve shown for death assumes pre-dive weight of 20 kg.

Table 1. Summary of severe DCS distribution and onset

Depth, fsw	Weight, kg	n	DCS			Time of Onset, min	No. Died	Time of Death, min
			CNS	CP	Both			
50	20.30 ± 1.47	4						
60	19.90 ± 0.50	4						
70	19.30 ± 1.45	4						
80	19.22 ± 1.56	6						
90	21.15 ± 1.40	6	3			19.00 ± 1.00		
95	19.64 ± 1.61	7	2	1	1	18.75 ± 8.54	2	38.00 ± 2.83
100	19.52 ± 1.32	10	4		2	25.20 ± 15.19*	2	34.00 ± 22.63
105	20.57 ± 1.86	6	3	1		22.50 ± 11.90	1	39
110	20.47 ± 1.86	44	14	3	13	21.33 ± 15.41	11	31.18 ± 10.27
115	20.60 ± 1.48	4			3	12.00 ± 13.08	2	32.50 ± 10.61
120	18.05 ± 0.73	4		1	2	14.67 ± 4.62	1	23
130	19.69 ± 1.37	12	2	5	4	17.00 ± 16.09	7	22.71 ± 5.65
140	21.13 ± 1.26	9		6	3	10.67 ± 3.32	9	20.22 ± 14.11
150	18.46 ± 1.77	8		6	2	12.25 ± 6.52	8	20.88 ± 12.15

Values are means ± SD. Number, distribution, and mean time of onset of severe decompression sickness (DCS) and death are shown for each of the profiles tested. *n*, Number of animals at a specified depth; DCS, number of animals diagnosed with severe DCS, divided into central nervous system cases (CNS), cardiopulmonary cases (CP), or both. *Mean calculated minus the 1 animal with CNS DCS onset >4 h after surfacing.

imals with cardiopulmonary DCS recovered (18.9%). If the animal did not recover, it manifested central cyanosis and increasing respiratory distress, eventually declined into agonal respiration, and then died. All deaths were due to cardiopulmonary DCS.

Skin DCS. Skin DCS was also common in this model (103 of 128 animals). Clinically it resembled previous descriptions in the literature of a slowly expanding, blanching erythematous discoloration that matured into a violaceous nonblanching fixed lesion (5). Its presence and speed of appearance correlated with depth ($R = 0.36$, $P \leq 0.001$ for both), but the rate of spread and final surface area varied between animals. The histopathology of skin DCS in this model has been described elsewhere (6). The presence and the speed of skin DCS onset were not correlated with eventual outcome.

Pathological findings. On necropsy, animals that died from DCS demonstrated marked pulmonary mottling and edema and copious intravascular bubbles distributed throughout the vena cavae, right heart, and pulmonary venous circulation. No patent foramina

ovale were discovered, and no arterial bubbles were noted. Gross spinal cord hemorrhages were discovered in six animals; these hemorrhages did not significantly correlate with a diagnosis of neurological DCS or with final outcome. Microscopically, mild-to-moderate multifocal hemorrhages with gliosis and perivascular cuffing were noted in the brain and spinal cord, with slightly increased incidence in the cervical cord, mid-brain, and frontal cortex. Animals that survived their severe DCS had no observed intravascular bubbles but did have similar histological CNS findings and some pulmonary mottling and edema, albeit to a lesser extent than those animals that died acutely. No clear correlation between histopathology and outcome could be demonstrated.

DISCUSSION

The US Navy has not had to rescue submariners since the USS Squalus sank in 1939. However, as long as submarine operations continue, such situations remain plausible, especially since the United States now maintains rescue assistance agreements with >20 countries. Many of these countries operate primarily in littoral waters, making the possibility of rescue operations all the more likely.

Outcome criteria in this study (clear neurological dysfunction and marked cardiorespiratory compromise) were necessarily severe, in part because the more subtle manifestations of the disease often cannot reliably be detected in an animal model. The need to observe the untreated natural history of the disease precluded use of more invasive and, therefore, more sensitive testing methods. This was in turn prompted by the very real possibility that a recompression chamber may not be available at a disabled submarine rescue site. The question to be answered was not how many subjects could benefit from recompression; theoretically all could. Instead, we chose criteria designed to characterize how many subjects would require a

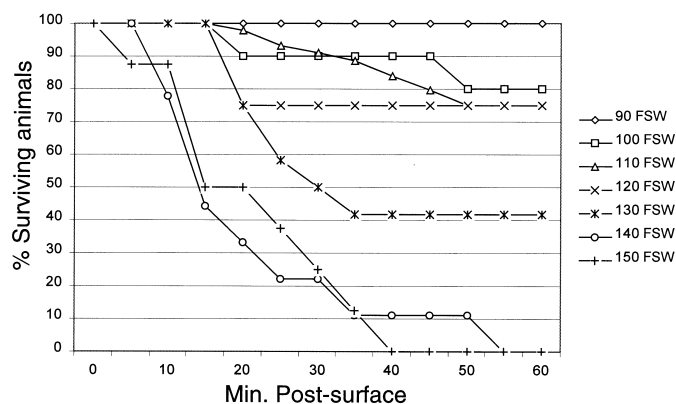


Fig. 3. Survival curves. Percentage of surviving animals is shown as a function of time for the various dive profiles. As depth increases, the latency and overall survival decrease.

Table 2. *Logistic regression analysis*

Variable	Univariate Analysis		Preliminary Model		Final Model	
	β_n	<i>P</i>	β_n	<i>P</i>	β_n	<i>P</i>
<i>Severe DCS</i>						
Intercept			-8.39 ± 1.837	<0.0001	-8.33 ± 1.909	<0.0001
Age	-0.004 ± 0.027	0.8694				
Preweight	0.142 ± 0.110	0.1975	0.213 ± 0.141	0.1293		
Weight loss	0.303 ± 0.272	0.2647				
Depth	0.087 ± 0.018	<0.0001	0.088 ± 0.018	<0.0001	0.083 ± 0.018	<0.0001
<i>Death</i>						
Intercept			-17.91 ± 4.060	<0.0001	-10.57 ± 4.10	<0.0001
Age	-0.029 ± 0.030	0.3235				
Preweight	0.135 ± 0.110	0.2213	0.279 ± 0.142	0.0498	0.305 ± 0.140	0.0361
Weight loss	0.582 ± 0.302	0.0542	0.272 ± 0.401	0.4980		
Depth	0.095 ± 0.018	<0.0001	0.100 ± 0.020	<0.0001	0.088 ± 0.020	<0.0001

Values are means \pm SE. β_n , parameter associated with the respective variable. Analysis was conducted using logistic regression with maximum-likelihood parameter estimation in the manner described by Hosmer and Lemeshow (17). After univariate analysis, all variables with $P \leq 0.25$ were incorporated into the preliminary model, which was then subjected to likelihood ratio testing to determine individual variable significance. All remaining variables with $P < 0.05$ were then included in the final model used to generate dose-response curves for each outcome.

chamber to prevent CNS morbidity or life-threatening DCS.

Swine have well-recognized anatomic and physiological similarity to humans, and volumes have been written about their utility as biomedical research models (15, 19, 27). In recent years they have been successfully used to study a variety of diving-related conditions (4–6, 9, 22). They are common domestic animals, and the use of matched littermate pairs from a closed breeding colony minimizes genetic variability. These facts, combined with their ease of handling, make them very useful in DCS experimentation. The pathological findings of livid skin DCS, multiple punctate spinal and cerebral hemorrhages, and profuse pulmonary congestion after no-stop decompression are consistent with previous observations in other animal models of DCS, as well as human results (7, 8, 14, 30).

Appropriate application of Monte Carlo simulation before the experiment maximized efficiency. By using a group size and depth selection rules designed to converge on a specific incidence, we localized the desired dose point within 40 animals (see APPENDIX). The initial dose-response curve with 40 animals predicted 75% incidence at 108.5 fsw (4.29 ATA). The final curve with 128 animals, including 36 additional dives in the region of specific interest, predicted 75% incidence at 112 fsw (4.39 ATA), <4 fsw from the first estimate. Had we been restricted to the original cohort of 40, we would still have correctly determined that the dose response had a steep slope with the desired dose point at or near 110 fsw (4.33 ATA). Targeting the desired dose point early allowed us to concentrate more than one-third of our total sample size in higher incidence regions. Confidence intervals around the 70–75% incidence region are much narrower than would have been achieved by distributing animal dives evenly across the entire depth range, resulting in a well-defined historical control group for ongoing interventional studies. Confronted with a paucity of background data, pretrial

Monte Carlo simulations provided an efficient way to proceed with a limited sample size and better allocation of animals within the final larger sample size. When used in human dive trials, comparable pretrial statistical modeling produces dramatic reductions in experimental cost, duration, and overall subject requirement (25).

The model provides a new tool for prospective evaluation of factors and treatment interventions that may affect DCS. The resulting depth-based dose-response curve describes the natural history of DCS in regions too severe for human testing. Because depth is the one significant variable that changes incidence, the model can be easily manipulated to produce specific amounts and/or types of DCS. Although it does not achieve significance, there is a trend for increasing animal weight to increase the risk of DCS. Lillo et al. (18) found a stronger weight dependence in rats, presumably because of a wider relative weight range. Neither age nor weight change during the dive (a surrogate for respiratory and urinary fluid losses) was significant here.

Besides producing information about severe DCS incidence after air saturation, this trial revealed important facts about DCS character as well. In shallower depths, CNS symptoms predominate, but as depth increases there is a gradual shift to the more fulminant cardiopulmonary DCS that rapidly becomes fatal. This finding has medical and logistical relevance for rescue planners. Well-documented human data on air saturation are limited to depths <30 fsw (1.91 ATA) with apparent and statistically estimated incidence rates well below 50% (28). Human DCS symptoms in that range are mostly pain only, with a few paresthesias, symptoms difficult to detect in swine. If the two species react similarly, the severe CNS symptoms and especially the fatal cardiopulmonary DCS must occur in humans at depths >30 fsw (1.91 ATA). Spontaneous recovery from relatively minor symptoms has been

observed in humans, but recovery from more severe symptoms cannot be assessed because such experimental cases are immediately treated. We were surprised at the frequency of spontaneous and complete reversal of serious neurological and cardiopulmonary manifestations in the swine model, although relapse beyond 24 h or more subtle persistent residual problems cannot be ruled out. Perhaps the human capacity for recovery without recompression therapy is greater than presently estimated, as evidenced by some anecdotal reports (16, 31). Even at very severe incidence levels, some animals showed no evidence of DCS. The only constant in DCS research remains its mystifying variability.

So what do these results mean for human DCS after long air exposures? They present a quantitative caution for human DCS modeling. The best-characterized human models extrapolate from the low-dose data with a shallower dose-response curve than the swine demonstrate (21, 26). The predicted human curve extends from 25 to 75% incidence over a depth range of 40–120 fsw (2.21–4.64 ATA), slightly more than a doubling in pressure. Swine incidence increases from 25 to 75% over a range of 87–112 fsw (3.64–4.39 ATA), only a 17.1% pressure increase. DCS risk in rodents, the only other extensively studied species, rises from 25 to 75% in about a 30% absolute pressure increase (18). Taken together, the animal observations strongly suggest

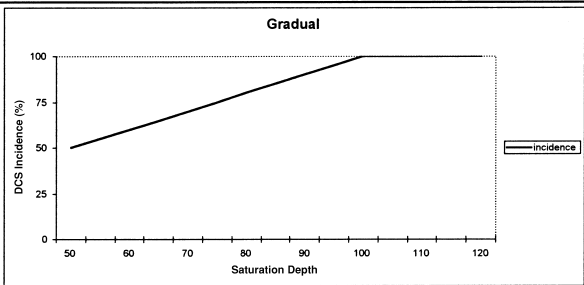
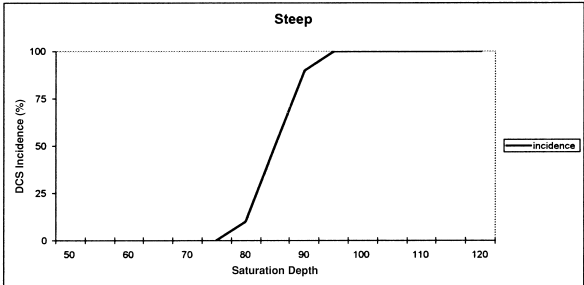
that existing human DCS models may severely underestimate human incidence predictions from deeper saturation depths, and nothing in modeling human-only data predicts the cardiopulmonary fatalities observed in swine and rodents when DCS incidence exceeds 50%. The probable extrapolation error of human-only modeling can be readily understood as an inability to observe some of the more severe manifestations of the disease at the available, and ethical, lower human doses. These findings warrant a more formal mathematical analysis of the cross-species data, as has recently been demonstrated to be feasible for shorter human and sheep exposures (1).

APPENDIX

Trial design and dive profile selection. No reports on saturation dives with swine could be found in the literature. Lillo et al. (18) developed a complete dose-response curve for rodents that had a steep, sigmoidal shape, but very little work had been done on saturation dives for larger animals. On the basis of log-log correlation of different species, Flynn and Lambertsen (13) estimated a 50% incidence at 61 fsw (2.85 ATA) for a 20-kg animal, whereas the estimate of Berghage et al. (3) using similar methods was 84 fsw (3.55 ATA).

Initially, 24 animals were allotted to the study, to be used to find a high-incidence dose point defined as 75% DCS. With so little starting information and such a limited cohort, the greatest potential problem was completing the entire trial

Table 3. Results of Monte Carlo simulations

Assumed Underlying Curve	Group Size	Average Distribution of 24 Animals, by incidence		
		<49%	50–90%	90–100%
	<i>n</i>	<49%	50–90%	90–100%
	8	<1	23	<1
	4	<1	23	<1
	<i>n</i>	<49%	50–90%	90–100%
	8	8	8	8
	4	11	5.4	7.6
	2	5.8	11.2	7.0

Average distribution of animals in relation to incidence regions on the assumed underlying dose-response curve after 2,000 iterations of Monte Carlo simulation are shown. Each run used a cohort of 24 animals and a predefined set of decision rules that changed depths on the basis of the outcomes after every 8, 4, or 2 animals. Success of any set of rules was assessed by noting the average total number of animals exposed in the middle region, near the desired 75% incidence point on an assumed dose-response curve. If the underlying dose-response curve is gradual, then all 3 methods are almost equally successful. However, if the underlying dose-response curve is steep, then changing depths after 2 animals is the most successful method of exploration.

with no animals exposed near the desired 70–75% range. Such all-or-none outcomes could arise if the starting depth was a poor choice and the trial rules were too inflexible to move quickly to a more appropriate depth. Fixed rules using only predetermined depths were abandoned, because incorrect starting depths could waste the entire cohort of animals. Adaptive rules were needed, such that once a group of animals was exposed, the next test depth would be based on the observed outcome of the prior group, both in magnitude and direction of change.

The number of possible trial rules is daunting. One can change starting depth, depth step size(s), or group size, and all may interact differently with the underlying dose-response curve. We simulated starting at a depth near the desired point, as well as too high and too low. We briefly explored using a single step size; for example, if group incidence was <70–75% DCS, we would then expose the next group 20 fsw deeper. Most simulations, however, used a proportional step size chosen by the following formula

$$\text{Step} = -10 \text{ fsw} * (\text{no. of DCS} - 0.75 * n)$$

where no. of DCS is the number of DCS cases observed in a given group size n . This process selected the next depth on the basis of how closely the prior group's outcome approached the desired dose point. For example, suppose group size was set at four animals. Then a "perfect" incidence would have 75%, or three of four animals. The depth step for the next group would be 0 fsw; we would use the next group at the same depth. If the outcome were two of four animals, we would subject the next group to a dive 10 fsw deeper. If only one of four suffered DCS, the next depth would be 20 fsw deeper, and if outcome was zero of four, the next depth would be 30 fsw deeper. If all animals got DCS, then the next exposure would be 10 fsw shallower.

Repeated rounds of Monte Carlo simulation were used to find the most efficient and robust experimental design (12, 23, 24). First, one of six different underlying dose-response curves was assumed. Then a set of possible group sizes was chosen where the depth change was invoked after eight, four, or even two animals per depth. For a particular assumed dose response and group size, a pseudorandom number generator simulated the course of a full 24-animal trial. Simulations used 50 fsw (2.52 ATA) as the starting depth and a variable step size of 10 fsw times the number of animals away from the desired outcome, as described above. Simulations typically used 2,000 runs to ensure acquisition of a stable average distribution, which was then plotted against depth. Success of any set of rules was assessed by noting how many of the animals, on average, were exposed near 70–75% incidence on the assumed dose-response curve.

Table 3 illustrates some of the lessons learned. Two underlying dose-response curves are presented: one gradual (e.g., the USN 93 model predictions) and one steep (e.g., the rodent data). For both, the 75% target is somewhat deeper than the starting depth. For the gradual curve, the adaptive rules worked well regardless of group size. Nearly all animals were, on average, exposed near the desired incidence. For the steep curve, however, group size was an important factor. Larger group sizes tended to oscillate above and below the target incidence, instead of converging on the desired point. Using a small group size ($n = 2$) exposed the most animals near the desired incidence and was therefore the most successful approach. The advantage of smaller group size improved in larger trials. For example, in a simulation with 60 animals and a steep dose-response curve with $n = 2$, ~70% of the animals were clustered around the desired high-incidence point (data not shown).

On the basis of these simulations, several decisions were made. First, the trial would use a depth change rule based on outcomes from only two animals. For a steep dose-response curve this group size proved most efficient, despite the counterintuitive nature of acting on such seemingly limited information. Second, a starting depth of 80 fsw (3.42 ATA) was chosen to be on the high end of the 50% incidence estimates from the literature. Third, because simulations proved the benefit of a larger cohort, the resource plan was modified to acquire 40 animals. As seen above, that sample size described basic curve shape and found the high-incidence dose point with marked efficiency.

We are indebted to Catherine Jones, Melvin Routh, Chief Petty Officers Tony Ruopoli and Rob Hale, and Petty Officers Harold Boyles, William Dow, Thomas Robertson, and Norman Wilt for excellent technical assistance during the experiments; the staff of the Laboratory Animal Medicine and Science Department and Technical Services Department at the Navy Medical Research Center; and Susan Mannix and Diana Temple for help in preparation of the manuscript.

This work was supported by Naval Sea Systems Command work unit 63713N M000099.01B-1610.

The opinions and assertions contained herein are the private ones of the authors and are not to be construed as official or reflecting the views of the Navy Department or the naval service at large.

REFERENCES

1. **Ball R, Lehner CE, and Parker EC.** Predicting risk of decompression sickness in humans from outcomes in sheep. *J Appl Physiol* 86: 1920–1929, 1999.
2. **Behnke A.** *Early Quantitative Studies of Gas Dynamics in Decompression.* Baltimore, MD: Williams & Wilkins, 1975.
3. **Berghage TE, David TD, and Dyson CV.** Species differences in decompression. *Undersea Biomed Res* 6: 1–13, 1979.
4. **Broome JR.** Reduction of decompression illness risk in pigs by use of non-linear ascent profiles. *Undersea Hyperb Med* 23: 19–26, 1996.
5. **Broome JR and Dick EJ Jr.** Neurological decompression illness in swine. *Aviat Space Environ Med* 67: 207–213, 1996.
6. **Buttolph TB, Dick EJ Jr, Toner CB, Broome JR, Williams R, Kang YH, and Wilt NL.** Cutaneous lesions in swine after decompression: histopathology and ultrastructure. *Undersea Hyperb Med* 25: 115–121, 1998.
7. **Catron PW, Flynn ET Jr, Yaffe L, Bradley ME, Thomas LB, Hinman D, Survanshi S, Johnson JT, and Harrington J.** Morphological and physiological responses of the lungs of dogs to acute decompression. *J Appl Physiol* 57: 467–474, 1984.
8. **Cole C, Chamberlain D, Burch B, Kempf J, and Hitchcock F.** Pathological effects of explosive decompression to 30 mmHg. *J Appl Physiol* 6: 96–104, 1953.
9. **Dick, EJ Jr, Broome JR, and Hayward IJ.** Acute neurologic decompression illness in pigs: lesions of the spinal cord and brain. *Lab Anim Sci* 47: 50–57, 1997.
10. **Eckenhoff R and Osborne S.** Direct ascent from shallow air saturation exposures. *Undersea Biomed Res* 13: 305–316, 1986.
11. **Eckenhoff RG and Parker JW.** Latency in onset of decompression sickness on direct ascent from air saturation. *J Appl Physiol* 56: 1070–1075, 1984.
12. **Fishman GS.** *Monte Carlo: Concepts, Algorithms, and Applications.* New York: Springer, 1997.
13. **Flynn E and Lambertsen C.** Calibration of inert gas exchange in the mouse. In: *Underwater Physiology IV*, edited by C. Lambertsen. New York: Academic, 1971, p. 179–191.
14. **Ghose N.** Death from compressed air sickness in India. *Indian Med Gaz* 14: 698–699, 1930.
15. **Hannon J.** Hemodynamic characteristics of the conscious resting pig: a brief review. In: *Swine in Biomedical Research*, edited by M. Tumbleson. Columbia, MO: Plenum, 1986, p. 1341–1353.
16. **Hill L.** *Caisson Sickness and the Physiology of Work in Compressed Air.* New York: Longmans, Green, 1912, p. 63–64.

17. **Hosmer W and Lemeshow S.** *Applied Logistic Regression*. New York: Wiley, 1989.
18. **Lillo RS, Flynn ET, and Homer LD.** Decompression outcome following saturation dives with multiple inert gases in rats. *J Appl Physiol* 59: 1503–1514, 1985.
19. **McKiennan R.** Exercise and hemodynamic studies in swine. In: *Swine in Cardiovascular Research*, edited by H. Stanton. Boca Raton, FL: CRC, 1986, p. 105–120.
20. **National Research Council.** *Guide for the Care and Use of Laboratory Animals*. Washington DC: National Academy Press, 1996.
21. **Parker EC, Survanshi SS, Massell PB, and Weathersby PK.** Probabilistic models of the role of oxygen in human decompression sickness. *J Appl Physiol* 84: 1096–1102, 1998.
22. **Reinertsen RE, Flook V, Koteng S, and Brubakk AO.** Effect of oxygen tension and rate of pressure reduction during decompression on central gas bubbles. *J Appl Physiol* 84: 351–356, 1998.
23. **Rubinstein RY.** *Simulation and the Monte Carlo Method*. New York: Wiley, 1981.
24. **Sobol IM.** *A Primer for the Monte Carlo Method*. Boca Raton, FL: CRC, 1994.
25. **Survanshi S, Parker E, Gummin D, Flynn E, Toner C, Temple D, Ball R, and Homer L.** *Human Decompression Trial With 1.3 ATA Oxygen in Helium*. Bethesda, MD: Naval Medical Research Institute, 1998. (Tech. Rep. 98-09)
26. **Survanshi S, Parker E, Thalmann E, and Weathersby P.** *Statistically Based Decompression Tables XII*. Bethesda, MD: Naval Medical Research Center, 1997. (Tech. Rep. 97-36)
27. **Swindle M.** *Swine as Models in Biomedical Research*. Ames, IA: Iowa State University Press, 1992.
28. **Temple D, Ball R, Weathersby P, Parker E, and Survanshi S.** *The Dive Profiles and Manifestations of Decompression Sickness Cases After Air and Nitrogen-Oxygen Dives. Data Set Summaries, Manifestations, Descriptions, and Key Files*. Bethesda, MD: Naval Medical Research Center, 1999, vol. I. (Tech. Rep. 99-02)
29. **VanDerAue O, Kellar R, and Brinton E.** *The Effect of Exercise During Decompression From Increased Barometric Pressures on the Incidence of Decompression Sickness in Man*. Washington, DC: Dept. of the Navy, 1949. (Navy Experimental Diving Unit Rep. 8-49)
30. **VanRensselaer H.** The pathology of the caisson disease. *Med Rec NY* 40: 141–150, 178–182, 1891.
31. **Woodward C.** *A History of the St. Louis Bridge*. St. Louis, MO: GI Jones, 1881.

